Contribution from the Department of Chemistry,
The University of North Carolina at Chapel Hill, Chapel Hill, North Carolina 27599-3290

Magnetic and Structural Properties of $[Cu(dien)OAc]_n(ClO_4)_n$: A μ-Acetato-Bridged Quasi-One-Dimensional Complex

Debra K. Towle,[1a] S. K. Hoffmann,[1b] William E. Hatfield,*[1a] Phirtu Singh,[1c] and Phalguni Chaudhuri[1d]

Received December 5, 1986

The complex formulated as [Cu(diethylenetriamine)(CH_3COO)](ClO_4) crystallizes in the space group $P2_1/n$ with $Z = 4$. A single-crystal X-ray diffraction study revealed chains of acetate-bridged copper(II) ions along the *b* crystal axis. Magnetic susceptibility data were collected in the temperature range 1.8–60 K. There is an increase in the magnetic moment below 10 K, with a maximum value and subsequent abrupt decrease in magnetic moment occurring at 2.3 K. Magnetic susceptibility data in the temperature range 5–60 K were fit with the Baker expansion for ferromagnetic chains, which is based on the high-temperature Padé expansion technique. The best fit was found with $J = 0.52$ cm^{-1}, $zJ' = -0.30$ cm^{-1}, and $g = 2.18$. Single-crystal EPR data were collected and analyzed. The line shapes are Lorentzian in all orientations of the crystal, which suggests significant interchain spin diffusion. Such interchain interactions may lead to a magnetic phase transition, as suggested by the abrupt change in magnetic moment at 2.3 K. A plot of the angular dependence of the line width shows minima at approximately 55° from the chain axis. This is a typical result for a quasi-one-dimensional complex.

Introduction

In view of the magnetic properties of the linear chain compound aqua[*N*-(salicylaldimino)glycinato]copper(II) hemihydrate (CuNSG),[2] which are consistent with a spin Peierls transition,[3] other mono(μ-carboxylate)-bridged copper(II) chain compounds are of interest. Such compounds may also exhibit similar magnetic behavior and permit magnetostructural correlations to be derived. In the course of a systematic study of the magnetic and structural properties of dimeric copper(II) complexes with the formula $[Cu(diethylenetriamine)X]_2Y_2$,[4-7] the complex formulated as [Cu(dien)(CH_3COO)](ClO_4) was investigated. Magnetic studies indicated a ferromagnetic exchange interaction in the complex, which is also the case for $[Cu(dien)Cl]_2(ClO_4)_2$[4,5] and $[Cu(dien)Br]_2(ClO_4)_2$.[6] The single-crystal EPR spectra, however, suggested that this complex was not dimeric, but, instead, one-dimensional. This prompted an investigation of the crystal and molecular structure of [Cu(dien)OAc](ClO_4), which revealed chains of mono(μ-acetate)-bridged copper(II) ions separated by perchlorate anions.

Acetate and other (O–C–O) ligands are known to assume many types of bridging conformations. The following important types are shown:

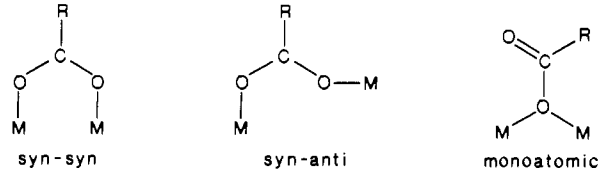

Copper acetate monohydrate is dimeric with four syn-syn acetate bridges between the copper(II) ions.[7] The syn-syn conformation gives rise to small Cu–Cu distances. The chain complex $[Cu_2(OAc)_2A]_n(ClO_4)_{2n}$ (A = 1,4,7,13,16,19-hexaaza-10,22-dioxacyclotetracosane) contains copper ions that are alternatingly bridged by two syn-anti acetate bridges and by the macrocyclic ligand, A.[8] It is interesting to note that the non-acetate copper coordination sites are occupied by three nitrogen atoms from the macrocycle, since this type of ligation is similar to that in [Cu(dien)OAc](ClO_4). Another type of acetate-bridged copper complex with a tridentate ligand is $[Cu(AE)OAc]_2$ (AE = 7-amino-4-methyl-5-aza-3-hepten-2-onate).[9] This dimeric complex contains copper ions that are bridged by two acetate ligands in the monoatomic conformation.

Here, the results of structural, magnetic susceptibility, and EPR studies on [Cu(dien)OAc](ClO_4) are described and related to those from other acetate- and (O–C–O)-bridged Cu(II) complexes.

Table I. Crystallographic Data for [Cu(dien)(OAc)](ClO_4)

a	10.138 (5) Å	space group	$P2_1/n$
b	8.064 (4) Å	μ(Mo K_α)	19.76 cm^{-1}
c	15.536 (10) Å	D_{calcd}	1.72 g/cm^3
β	99.00 (4) Å	collimator size	1.5 mm
V	1254.5 Å^3	no. of observns	1077
Z	4	no. of vars	154
R	0.058	esd of an observn of unit wt	2.25
R_w	0.051		

Experimental Section

Synthesis of [Cu(dien)OAc](ClO_4). Diethylenetriamine (1 g, 10 mmol) was added with constant stirring to a solution of 2.0 g $Cu(CH_3CO-O)_2 \cdot H_2O$ (10 mmol) in 40 mL of water at 50 °C, and the stirring was continued for 0.5 h. Solid $NaClO_4 \cdot H_2O$ (1 g) was added to this deep blue solution, and the solution was filtered to remove any solid particles. The filtrate was kept at 5 °C for 4 h, whereupon deep blue crystals separated out. The crystals were collected by filtration, washed with an ethanol–diethyl ether mixture, and air-dried. Yield: 2.4 g. Anal. Calcd for $[Cu(C_4H_{13}N_3)(C_2H_3O_2)]ClO_4$: C, 22.16; H, 4.96; N, 12.92; Cu, 19.54; ClO_4, 30.58. Found: C, 22.34; H, 5.04; N, 13.1; Cu, 19.7; ClO_4, 30.7.

Suitable crystals for EPR and single-crystal X-ray diffraction measurements were obtained by slow recrystallization of the crude product from distilled water. All measurements were made by using crystals or powdered crystals from the same batch of recrystallization product.

Crystallographic Measurements. The crystals of the complex grow as long blue needles. They are difficult to cut since they split lengthwise. Therefore, a needle with approximate dimensions $1.0 \times 0.20 \times 0.15$ mm^3 was used. The crystal, mounted on a eucentric goniometer head, was transferred to a CAD-4 computer-controlled diffractometer equipped with a molybdenum tube and graphite monochromator. Cell parameters were obtained by least-squares refinement of the setting angles of 25

(1) (a) The University of North Carolina. (b) Institute of Molecular Physics, Polish Academy of Sciences, 60-179 Poznan, Poland. (c) North Carolina State University, Raleigh, NC. (d) Ruhr-Universität Bochum, Bochum, West Germany.
(2) Hatfield, W. E.; Helms, J. H.; Rohrs, B. R.; ter Haar, L. W. *J. Am. Chem. Soc.* **1986**, *108*, 542.
(3) (a) Bray, J. W.; Interrante, L. V.; Jacobs, I. S.; Bonner, J. C. In *Extended Linear Chain Compounds*; Miller, J. S., Ed.; Plenum: New York, 1982; Vol. 3 and references therein. (b) Jacobs, I. S.; Bray, J. W.; Hart, H. R.; Interrante, L. V.; Kasper, J. S.; Watkin, G. D.; Prober, D. E.; Bonner, J. C. *Phys. Rev. B: Solid State* **1976**, *14*, 3036. (c) Northby, J. A.; Groenendijk, H. A.; de Jongh, L. J.; Bonner, J. C.; Jacobs, I. S.; Interrante, L. V. *Phys. Rev. B: Condens. Matter* **1982**, *25*, 3215. (d) de Jongh, L. J. In *Magneto-Structural Correlations in Exchange Coupled Systems*; Willett, R. D., Gatteschi, D., Kahn, O., Eds.; Reidel: Dordrecht, Holland; 1985.
(4) Hoffmann, S. K.; Towle, D. K.; Hatfield, W. E.; Weighardt, K.; Chaudhuri, P.; Weiss, J. *Mol. Cryst. Liq. Cryst.* **1983**, *107*, 161.
(5) Hoffmann, S. K.; Towle, D. K.; Hatfield, W. E.; Chaudhuri, P.; Wieghardt, K. *Inorg. Chem.* **1985**, *24*, 1307.
(6) Towle, D. K., Hoffmann, S. K.; Hatfield, W. E.; Chaudhuri, P.; Singh, Phirtu; Wieghardt, K. *Inorg. Chem.* **1985**, *24*, 4393.
(7) Van Niekirk, J. N.; Schoening, F. K. L. *Acta Crystallogr.* **1953**, *6*, 227.
(8) Coughlin, P. K.; Lippard, S. J. *J. Am. Chem. Soc.* **1984**, *106*, 2328.
(9) Costes, J. P.; Dahan, F.; Laurent, J. P. *Inorg. Chem.* **1985**, *24*, 1018.

0020-1669/88/1327-0394$01.50/0

Table II. Positional Parameters of the Non-Hydrogen Atoms and Their Estimated Standard Deviations in Parentheses

atom	x	y	z
Cu	0.6988 (1)	0.3831 (1)	0.26549 (7)
Cl	0.1753 (2)	0.2543 (3)	0.4330 (2)
O(1)	0.2177 (8)	0.1269 (10)	0.3816 (5)
O(2)	0.0441 (7)	0.2188 (12)	0.4467 (6)
O(3)	0.2566 (6)	0.2566 (12)	0.5108 (4)
O(4)	0.1867 (10)	0.4040 (10)	0.3913 (5)
O(5)	0.8618 (5)	0.4387 (7)	0.2171 (4)
O(6)	0.8688 (5)	0.1654 (7)	0.2178 (4)
N(1)	0.5785 (6)	0.3888 (9)	0.1524 (4)
N(2)	0.5507 (6)	0.2674 (8)	0.3082 (4)
N(3)	0.7805 (6)	0.3934 (9)	0.3900 (4)
C(1)	0.4551 (9)	0.2850 (10)	0.1599 (6)
C(2)	0.4256 (8)	0.2990 (10)	0.2500 (6)
C(3)	0.5562 (8)	0.3080 (10)	0.4020 (6)
C(4)	0.6986 (8)	0.2930 (10)	0.4430 (5)
C(5)	0.9176 (8)	0.3010 (10)	0.2008 (5)
C(6)	1.04036 (8)	0.3080 (10)	0.1633 (6)

reflections with 2θ values higher than 30°. The intensity data were collected by the ω–2θ scan technique at a variable rate. Intensities of the three reflections were monitored every 3 h to check on crystal movement, decomposition, and instrument instability. Data were collected to 50° to 2θ and were corrected for Lorentz and polarization effects and for absorption. A small data set for the empirical absorption correction was collected. This consisted of ϕ scans for nine reflections with $\chi \geq 80°$. For each reflection, scans were started at $\Psi°$ and continued at 10° intervals so that a total of 37 scans were taken. Crystallographic data are given in Table I.

The structure was solved by the conventional heavy-atom method. The hydrogen atoms could not be located unambiguously from the difference Fourier map calculated by subtracting out all the other atoms. The hydrogen atoms in the dien ligand were, therefore, put in calculated positions with C–H = 1.00 Å and N–H = 0.95 Å. The methyl hydrogens were located in a subsequent difference Fourier map. The positions and the anisotropic factors of all the non-hydrogen atoms were refined by a full-matrix least-squares procedure using 1077 data with $F_o \geq 3\sigma$. The least-squares refinements were carried out on F with the function minimized being $\sum w(|F_o| - |F_c|)^2$ where $w = (4F_o^2)/[\sigma^2(I)]$. Near the end of the refinement it was observed that 13 reflections had rather high discrepancies between their observed and calculated F's. They were, therefore, removed from the final refinement, and the structure was refined to convergence. A final difference Fourier map was featureless with no peak higher than 0.2 Å^{-3}. All calculations, except those for structure illustrations, were performed on a PDP-11 computer using the structure determination package provided by the Enraf Nonius Corp. Structure illustrations were made by using ORTEP-II[10] on an IBM 360 computer.

The atomic coordinates derived from the final cycle of refinement along with their estimated standard deviations are given in Table II for the non-hydrogen atoms. Tables of hydrogen atom coordinates, atomic thermal vibrations, and calculated structure amplitudes are available as supplementary material.

Magnetic Measurements. Static magnetization data were collected on a powdered sample by using a Princeton Applied Research Model 155 vibrating-sample magnetometer (VSM) equipped with a Janis Research Co. liquid-helium dewar. The magnetometer was calibrated with Hg-Co(NCS)$_4$.[11] The VSM magnet (Magnion H-96), power supply (Magnion HSR-1365), and associated field control unit (Magnion FFC-4 with a Rawson-Lush Model 920 MCM rotating-coil gaussmeter) were calibrated against NMR resonances (^{1}H and ^{3}Li). A calibrated GaAs diode was used to monitor the sample temperature.

Magnetic susceptibility data were collected in the temperature range 1.8–60 K with a magnetic field of 10 kOe. Magnetization data were collected at 4.2 K in the magnetic field range 100–15000 Oe. The data were corrected to compensate for the diamagnetism of the constituent atoms and for the temperature-independent paramagnetism of the Cu(II) ions (60×10^{-6} cgsu).[12-15]

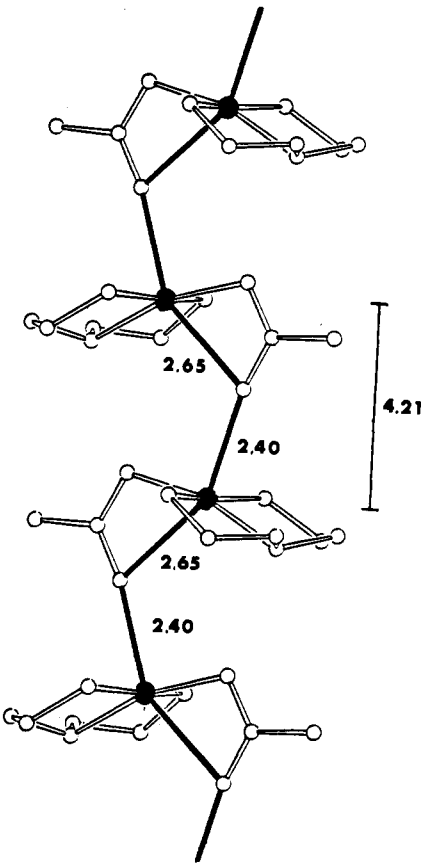

Figure 1. View of the chain running along the b axis of the crystal. Each monomeric unit in the chain is related to its neighboring unit by a 2-fold screw axis parallel to the b crystallographic axis.

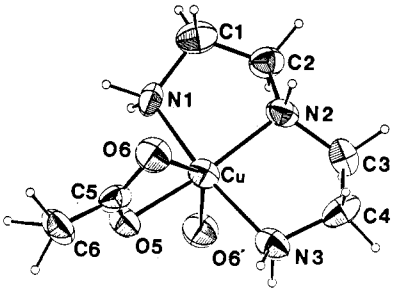

Figure 2. ORTEP[10] view of the cation [Cu(dien)OAc]$^+$ showing the distorted octahedral coordination around the copper atom. Non-hydrogen atoms are shown with 40% probability thermal ellipsoids, and hydrogen atoms, with circles of arbitrary size.

The exchange-coupling model described below was fit to the susceptibility data by using a nonlinear Simplex[16-18] fitting routine. The function minimized was

$$F = \sum_i \frac{(\chi_i^{obsd} - \chi_i^{calcd})^2}{(\chi_i^{obsd})^2}$$

Electron Paramagnetic Resonance. EPR spectra were recorded at X-band on a Varian E-109 spectrometer with a rectangular TE_{102} cavity. The magnetic field was calibrated with a DPPH marker, and the frequency was monitored with a Hewlett-Packard 5245L frequency counter. The spectra of a powdered sample enclosed in a quartz tube were obtained at room and liquid-nitrogen temperatures. The angular dependence of the single-crystal spectra was recorded at room temperature in

(10) Johnson, C. K. "ORTEP-II"; Report ORNL-5138; Oak Ridge National Laboratory: Oak Ridge, TN, 1976.
(11) Brown, D. B.; Crawford, V. H.; Hall, J. W.; Hatfield, W. E. *Inorg. Chem.* **1977**, *81*, 1303.
(12) McKim, F. R.; Wolf, W. P.; *J. Sci. Instrum.* **1957**, *34*, 64.
(13) Figgis, B. N.; Lewis, J., In *Modern Coordination Chemistry*; Lewis, J., Wilkins, R. G., Eds.; Interscience: New York, 1960; Chapter 6, p 403.
(14) Konig, E.; *Magnetic Properties of Transition Metal Compounds*; Landolt-Börnstein Series; Springer-Verlag: West Berlin, 1966.
(15) Weller, R. R.; Hatfield, W. E. *J. Chem. Ed.* **1979**, *56*, 652.
(16) Spendly, W.; Hext, G. R.; Himsworth, F. R. *Technometrics* **1962**, *4*, 441.
(17) Nelder, J. A.; Mead, R. *Computer J.* **1965**, *7*, 308.
(18) O'Neill, R. *Appl. Stat.* **1971**, *20*, 338.

Table III. Bond Disances and Bond Angles, with Esd's in Parentheses, Pertaining to the Copper Coordination Sphere

	Bond Distances, Å		
Cu–N(1)	1.976 (4)	Cu–O(6′)	2.403 (4)
Cu–N(2)	1.969 (5)	Cu–O(6)	2.646 (4)
Cu–N(3)	1.983 (5)	Cu···Cu	4.210 (4)
Cu–O(5)	1.972 (4)		
	Bond Angles, deg		
N(1)–Cu–N(2)	85.0 (2)	N(2)–Cu–O(6′)	99.6 (2)
N(1)–Cu–N(3)	166.3 (2)	N(3)–Cu–O(5)	96.6 (2)
N(1)–Cu–O(5)	95.4 (2)	N(3)–Cu–O(6)	96.3 (2)
N(1)–Cu–O(6)	96.0 (2)	N(3)–Cu–O(6′)	86.4 (2)
N(1)–Cu–O(6′)	85.8 (2)	O(5)–Cu–O(6)	54.7 (2)
N(2)–Cu–N(3)	85.1 (2)	O(5)–Cu–O(6′)	95.5 (2)
N(2)–Cu–O(5)	164.8 (2)	O(6)–Cu–O(6′)	150.2 (1)
N(2)–Cu–O(6)	110.1 (2)		

the orthogonal reference system $a^{\dagger}$, b, c, where b and c correspond to the respective crystallographic axes and the $a^{\dagger}$ axis is 9° from the crystallographic a axis in the ac plane.

Results and Discussion

Description of the Structure. The complex [Cu(dien)OAc]-(ClO_4) crystallizes in the monoclinic space group $P2_1/n$. There are four $[Cu(dien)OAc]^+$ cations and four perchlorate anions in the unit cell, which has the parameters a = 10.138 (5) Å, b = 8.064 (4) Å, c = 15.536 (10) Å, and β = 99.00 (4)°. The positional parameters of the non-hydrogen atoms are given in Table II. The equivalent positions in the space group $P2_1/n$ are x, y, z; $\bar{x}, \bar{y}, \bar{z}$; $^1/_2 + x, ^1/_2 - y, ^1/_2 + z$; and $^1/_2 - x, ^1/_2 + y, ^1/_2 - z$.

The crystal structure is composed of polymeric chains of $[Cu(dien)OAc]^+$ cations running parallel to the b axis, as shown in Figure 1. Each unit in the chain is related to the next by a 2-fold screw along the b axis. Every copper(II) ion is connected to two others in the chain by single syn-anti acetate bridges. The copper–copper distance is 4.21 Å and is uniform throughout the chain. The Cu–O(apical) distances alternate between 2.65 and 2.40 Å.

The structure of an individual $[Cu(dien)OAc]^+$ cation is shown in Figure 2. The coordination about copper is distorted 4 + 2 octahedral. The equatorial plane is composed of the three nitrogen atoms of the diethylenetriamine ligand and the O(5) atom of the acetate. The apical positions are occupied by the O(6) atom of the acetate ligand and the O(6′) atom from the acetate ligand of the next cation in the chain. Representative bond lengths and angles are given in Table III. The Cu–N and Cu–O(5) bond lengths are normal, but the Cu–O(6) and Cu–O(6′) distances are very long, as is expected for apical bond lengths in six-coordinate copper(II) complexes. The angles subtended by the ligating atoms differ markedly from 90 and 180°. This is due to the constraints of the tridentate diethylenetriamine and acetate ligand geometries. The distortion is especially severe for the acetate ligand, where the O(6)–Cu–O(5) angle is 55°. Further structural parameters will be discussed in the next section.

Magnetism. The results of susceptibility measurements for [Cu(dien)OAc](ClO_4) are shown in Figure 3. The magnetization as a function of applied field (100–15 000 Oe) at 4.2 K revealed a ferromagnetic exchange interaction; that is, the experimental magnetization was greater than predicted by the Brillouin function for $S = ^1/_2$. Because of this result, and the uniform chain structure of the complex, it was expected that the magnetic properties could be explained by the Heisenberg linear-chain model. The Hamiltonian for this type of exchange is

$$H_{ex} = -2J\sum_i S_i \cdot S_{i+1}$$

where J is the intrachain-exchange-coupling constant and the summation is over all members of the chain. When J is positive, the exchange is ferromagnetic.

The expression used to fit the data was that of Baker et al.,[19]

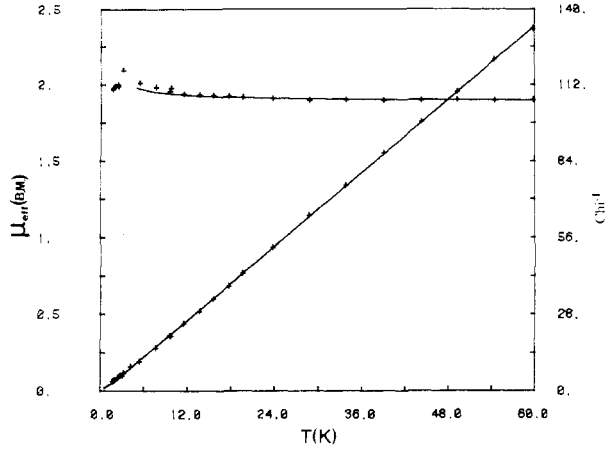

Figure 3. Plot of the magnetic moment and inverse magnetic susceptibility versus temperature for [Cu(dien)OAc](ClO_4). The solid lines were generated from the best-fit magnetic parameters as described in the text.

which is based on the high-temperature Padé expansion technique. The equation for a $S = ^1/_2$, ferromagnetic chain is

$$\chi_c = \left[\frac{1 + a_1K + a_2K^2 + a_3K^3 + a_4K^4 + a_5K^5}{1 + b_1K + b_2K^2 + b_3K^3 + b_4K^4}\right]^{2/3} \quad (1)$$

where $K = J/2k_bT$ and a_i and b_i are expansion coefficients. Interchain exchange was accounted for by the addition of a mean field correction term to eq 1. The equation for the susceptibility then has the form

$$\chi = \frac{\chi_c}{1 - 2zJ'\chi_c/Ng^2\mu_B^2} \quad (2)$$

χ_c is the susceptibility calculated from 1, J' is the interchain-exchange-coupling energy, and z is the number of nearest neighbors. The best fit of eq 2 to the data in the temperature range 5–60 K was found with J = 0.52 cm^{-1}, zJ' = −0.30 cm^{-1}, and g = 2.18. All three magnetic parameters were allowed to vary freely in the fitting calculations. The best fit for the g value is slightly higher than that obtained from the EPR measurements. The solid lines in Figure 3 show the results of the fitting calculations.

The higher temperature data correspond well with the theoretical predictions. However, for $T < 5$ K the data depart from the calculated values. Small deviations are expected since the accuracy of the ferromagnetic chain expression (eq 1) decreases as J/k_BT increases. However, the sharp discontinuity in the data for [Cu(dien)OAc](ClO_4) is of special interest with regard to transitions in copper chain compounds. The data points are reproducible. Below 2.3 K, the magnetic susceptibility continues to increase with decreasing temperature but μ_{eff} and $d\chi/dT$ decrease. This unusual behavior cannot be explained without additional magnetic data at even lower temperatures.

Mechanism of Exchange Coupling. The exchange coupling in acetate-, substituted-acetate-, and carbonate-bridged complexes is largely determined by the conformation of the bridge and the interaction between the d orbitals of the metal and the bridge. In complexes where the metal ions are bridged in a syn-syn manner, the exchange-coupling constant is large and antiferromagnetic. The dimeric complex[7,20] $Cu_2(OAc)_4 \cdot 2H_2O$ ($2J$ = −286 cm^{-1}) and the chain complex[19] bis(propionato)(*p*-toluidine)copper(II) (J = −105 cm^{-1}) are two examples of this type of bridging. In these complexes, the acetate ligands interact directly with the $d_{x^2-y^2}$ orbitals of the copper ions.

(19) Baker, G. A.; Rushbrooke, G. S.; Gilbert, H. E. *Phys. Rev.* **1964**, *135*, A1272.

(20) (a) Martin, R. L.; Watermann, R. *J. Chem. Soc.* **1957**, 2545. (b) Lewis, J.; Mabbs, F. E.; Royston, L. K.; Smail, W. R. *J. Chem. Soc. A* **1969**, 291.

(21) Yawney, D. B. W.; Moreland, J. A.; Doedens, R. J. *J. Am. Chem. Soc.* **1973**, *95*, 1164.

Table IV. Pertinent Cu–Cu and Cu–O(Perchlorate) Distances (Å) in [Cu(dien)OAc](ClO$_4$)

Cu(A)–Cu(B)[a]	4.21	Cu(A)–Cu(B′)	9.90
Cu(A)–Cu(C)	10.15	Cu(A)–Cu(C′)	8.85
Cu(A)–Cu(D)	9.06	Cu(A)–Cu(D′)	9.45
Cu(A)–Cu(A′)[b]	10.14	Cu(A)–Cu(A″)[c]	8.064
Cu(A)–O(4)	5.55	Cu(A)–O(1′)	4.89
Cu(C′)–O(4)	5.76	Cu(B′)–O(1′)	5.84

[a] Atoms are labeled as in Figure 2. [b] A′ = x_A + 1, y_A, z_A. [c] A″ = x_A, y_A + 1, z_A.

In complexes that contain syn-anti type bridges, the magnitudes of the exchange-coupling constants are smaller than those for the syn-syn-bridged complexes and the exchange is usually ferromagnetic.[8,22] The acetate ligand in [Cu(dien)OAc](ClO$_4$) assumes the syn-anti conformation, and the intrachain interaction is ferromagnetic in agreement with the other examples.[8,22] There are several possible contributions to the exchange interaction. These include superexchange involving the σ and π orbitals of the acetate bridge as well as the orbitals of O(6), which directly bridge adjacent copper ions through rather long bonds. Since the bonds to O(6) are long and are not directed toward the $d_{x^2-y^2}$ magnetic orbitals, exchange interactions by this pathway are probably minor. In view of the low site symmetry of the copper ion, it is difficult to attribute exchange interactions to a specific pathway. However, the dihedral angle between the plane of the acetate ligand and the plane containing the $d_{x^2-y^2}$ orbital is 90°, and this means that the π system of the acetate ligand is orthogonal to the $d_{x^2-y^2}$ orbitals. Superexchange interactions by orthogonal pathways yield ferromagnetic contributions. The σ orbital of O(6) in the apical position is also orthogonal to $d_{x^2-y^2}$, and superexchange through the σ system should also be ferromagnetic. Thus, [Cu(dien)OAc] is member of the limited class of compounds that exhibit ferromagnetic intrachain interactions.[23]

Interchain Interactions. The value of the ratio $zJ'/J = 0.59$ reflects the magnetic behavior that occurs at low temperature. First, there is an increase in the magnetic moment as a result of intrachain coupling, and this is followed by an abrupt decrease in moment presumably from interchain coupling. Such a large value would not be expected in view of the Cu–Cu interchain distance of 8.85 Å, but it is possible that some interchain interactions may arise from superexchange through the orbitals of the perchlorate oxygens. Relevant distances are shown in Table IV. The two shortest pathways for superexchange are Cu(A)–O(4)–Cu(C′) (path length 11.31 Å) and Cu(A)–O(1′)–Cu(B′) (path length 10.7 Å). Each copper has two of the former and one of the latter routes available for superexchange with a corresponding value of $z = 3$. There are several other slightly longer superexchange pathways available that make z even larger. Therefore, even though the intrachain coupling is expected to be small due to the long superexchange distances, the cumulative effect of these pathways could lead to a relatively large value of zJ'.

Other factors to consider here are the possible temperature dependences of the crystal structure and zJ'. In [Cu(dien)Cl]$_2$(ClO$_4$)$_2$,[2] J' was determined to decrease from 0.009 cm^{-1} at 93 K to 0.0018 cm^{-1} at 370 K. This temperature dependence of the interdimer coupling is throught to be due to a temperature dependence of the interdimer distance. The interstack-exchange coupling in $(C_7H_7)^+[Ni(mnt)_2]^-$ was found to have a similar temperature dependence.[24] The unit cell parameters of this complex decrease with decreasing temperatures. These results suggest that the room-temperature Cu–Cu and Cu–O(perchlorate) distances in [Cu(dien)OAc)(ClO$_4$) are different from, and most likely longer than, those in the temperature region (5.0–60 K) where zJ' was determined.

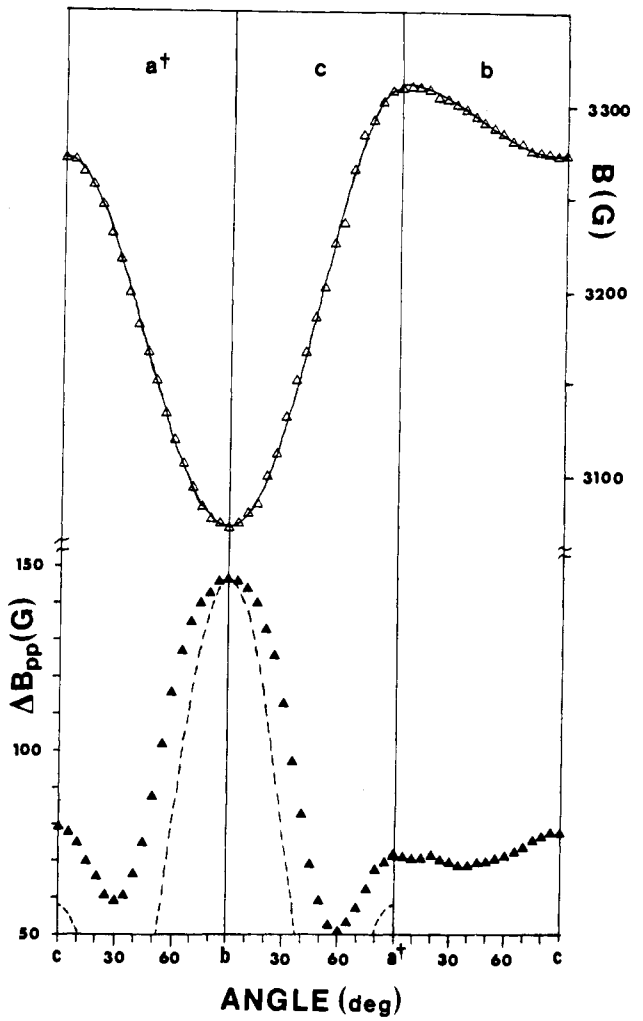

Figure 4. Plot of the angular dependence of B_0 (Δ) and the peak-to-peak line width ΔB_{pp} (▲) of the single-crystal EPR spectra of [Cu(dien)-OAc](ClO$_4$). The solid line represents the result of eq 4. The dashed line represents the result of eq 8.

Another possible contribution to zJ' is the exchange coupling between next-nearest neighbors in the chain. The Cu–Cu distance for this interaction is 8.064 Å at room temperature.

Electron Paramagnetic Resonance. The EPR spectra of a powdered sample of [Cu(dien)OAc](ClO$_4$) at room and liquid-nitrogen temperatures consisted of a single broad featureless band. Although there is some change in the line shape, there is no increase in resolution with temperature change.

The EPR spectra of a single crystal contain one Lorentzian line in all crystal orientations. The line widths vary from 51 to 147 G. Hyperfine splitting and zero-field splitting were not observed in the spectra in any crystal orientation. Hyperfine structure is not generally resolved in EPR spectra of magnetically condensed copper(II) compounds.

The angular dependences of the peak-to-peak derivative line width and B_0 are shown in Figure 4 for rotations about the orthogonal $a^\dagger$, b, and c axes, where b and c are the respective crystallographic axes and $a^\dagger = b \times c$. An angular g factor de-

(22) (a) Corvan, P. J.; Estes, W. E.; Weller, R. R.; Hatfield, W. E. *Inorg. Chem.* **1980**, *19*, 1297. (b) Gregson, A. K.; Moxon, N. T.; Weller, R. R.; Hatfield, W. E. *Aust. J. Chem.* **1982**, *35*, 1537.

(23) (a) Hirakawa, K.; Yamada, I.; Kurogi, Y. *J. Phys.* (*Les Ulis, Fr.*) **1971**, *32* (suppl.), 890. (b) Losee, D. B.; McElearney, J. N.; Siegel, A.; Carlin, R. L.; Khan, A. A.; Roux, J. P.; James, W. J. *Phys. Rev. B: Solid State* **1972**, *6*, 4342. (c) Swank, D. D.; Landee, C. P.; Willet, R. D. *Phys. Rev. B: Condens. Matter* **1979**, *20*, 2154. (d) Schouten, J. C.; Van der Geest, G. J.; De Jonge, W. J. M.; Kopinga, K. *Phys. Lett. A* **1980**, *78A*, 398. (e) O'sConnor, C. J.; Klein, C. L.; Majeste, R. J.; Trefonas, L. M. *Inorg. Chem.* **1982**, *21*, 64. (f) Willet, R. D.; Barberis, D.; Waldner, F. *J. Appl. Phys.* **1982**, *53*, 2677. (g) Kopinga, K.; Tinus, A. M. C.; De Jonge, W. J. M. *Phys. Rev. B: Condens. Matter* **1982**, *25*, 4685. (h) ter Haar, L. W.; Hatfield, W. E. *Mol. Cryst. Liq. Cryst.* **1983**, *107*, 171. (i) Caneschi, A.; Gatteschi, D.; Laugier, J.; Rey, P. *J. Am. Chem. Soc.* **1987**, *109*, 2191.

(24) Manoharan, P. T.; Noordik, J. H.; de Boer, E.; Keijzers, C. P. *J. Chem. Phys.* **1975**, *63*, 1926.

pendence in the ith crystal rotation can be described by the general $\mathbf{g}^2$ tensor expression[25,26]

$$g^2(i) = \alpha_i + \beta_i \cos 2\theta + \gamma_i \sin 2\theta \quad (3)$$

where θ is the azimuthal angle of the magnetic field. The anisotropy parameters α, β, and γ can be calculated by a least-squares method from a set of equidistant (in angle θ) experimental points from the expressions[27]

$$\alpha_i = n^{-1}\sum_{\theta=0}^{M} g^2(\theta)$$

$$\beta_i = 2n^{-1}\sum_{\theta=0}^{M} g^2(\theta) \cos 2\theta \quad (4)$$

$$\gamma_i = 2n^{-1}\sum_{\theta=0}^{M} g^2(\theta) \sin 2\theta$$

where $n = 36$, $M = 175°$ for data points collected in 5° intervals and $n = 18$, $M = 170°$ for 10° intervals. The $B(\theta)$ plots with parameters calculated from eq 4 are presented as solid lines in Figure 4, where a good fit to the experimental points may be seen. A collection of α, β, and γ parameters for three orthogonal rotations enables the determination of the $\mathbf{g}^2$ tensor components. The following g factors were obtained from the rotational data for [Cu(dien)OAc](ClO_4)

$$g_b = 2.212\ (1) \qquad g_c = 2.077\ (1) \qquad g_{a^\dagger} = 2.052\ (1)$$

Lines Shapes. EPR theory for one-dimensional complexes[28] predicts that the spectral line shape be non-Lorentzian when the applied field is parallel to the chain axis. This is due to long-time spin diffusion effects along the chain, which result in a line shape described by the Fourier transform of an exponential relaxation function with $(-t^{3/2})$ time dependence. This effect has been seen in the spectra of the "good" one-dimensional complex $(CH_3)_4N$-$MnCl_3$ (TMMC).[29]

In the case of [Cu(dien)OAc](ClO_4), the line shapes of the resonances do not vary from Lorentzian in any crystal orientation. One reason for this behavior could be the presence of interchain spin diffusion.

The interchain-coupling constant, J', has been used as a measure of the magnitude of off-chain spin diffusion.[30-32] Complexes with values of J'/J even smaller than 10^{-2} are known to have Lorentzian line shapes in all crystal orientations. Therefore, in view of the magnitude of J'/J, it is not surprising that the single-crystal EPR spectra of [Cu(dien)OAc](ClO_4) do not show the line shapes expected for purely one-dimensional magnetic interactions.

Line Widths. The line width in one-dimensional complexes is predicted to be proportional to

$$\Delta H_{pp} \propto \langle H^2 \rangle^{3/2}/|J|^{1/3} \quad (5)$$

where $\langle H^2 \rangle$ is the second moment of the EPR absorption and J is the intrachain-exchange-coupling frequency. Dipolar coupling, anisotropic exchange, and hyperfine coupling are some of the possible contributions to the second moment. In complexes such as [Cu(dien)OAc](ClO_4), anisotropic exchange and hyperfine coupling contributions to the second moment are less than those from dipolar coupling. The secular dipolar coupling contribution to the second moment can be expressed as

$$\langle H^2 \rangle_{dip} \propto \sum_{ij}(3 \cos^2 \phi_{ij} - 1)^2 (r_{ij})^{-6} \quad (6)$$

where r_{ij} is the distance between the ions and ϕ_{ij} is the angle between the vector $\mathbf{r}_{ij}$ and the magnetic field direction.

In one-dimensional complexes, dipolar coupling is expected to be largest between nearest neighbors in the chain due to their close proximity. Therefore, $\langle H^2 \rangle_{dip}$ and, as a consequence, the line width should be greatest for $\mathbf{H}$ along the chain axis. If the interchain distances are long compared to the interchain nearest-neighbor distances, and the angle between the vector $\mathbf{r}_{i,i+1}$ and the chain axis is very small, then the angular dependence of the line width is approximated by

$$\Delta H_{pp} \propto |3 \cos^2 \theta - 1|^{4/3} \quad (7)$$

where θ is the angle between the chain axis and the applied field. This expression predicts a line width of zero for $\theta = 54.7°$, the "magic angle". However, at angles close to 54.7°, nonsecular contributions to the second moment become important and give line widths that are greater than those expected.

In TMMC,[29] the ratio of intrachain to interchain nearest-neighbor distances is 0.36 and the Mn ions lie directly on the chain axis. The angular dependence of the line width is described (in gauss) by $540|3 \cos^2 \theta - 1|^{4/3}$, except in the region $\theta \sim 54.7°$ for the reason explained above.

The angular dependence of the line width for [Cu(dien)-OAc](ClO_4) is shown in Figure 4. The line width has a maximum value of 147 G at $\theta = 0°$ and minima of 51 and 59 G at $\theta \sim 60°$. The dashed line in Figure 4 shows the angular dependence of the line width calculated from eq 8, which is analogous to the ex-

$$\Delta H_{pp}\ (G) = 58.3|3 \cos^2 \theta - 1|^{4/3} \quad (8)$$

pression used to describe the line width behavior in TMMC.[29] The experimental line widths show relatively small differences from the calculated values.

There are two major reasons why these differences occur. First, the ratio of the intrachain to interchain nearest-neighbor distances in [Cu(dien)OAc](ClO_4) is 0.48. This suggests that interchain coupling is more important in this complex than in TMMC. However, the small (<10 G) variation in the angular dependence of the line width in the $a^\dagger c$ plane from the expected dependence suggests that the interchain dipolar contributions to the second moment are much less than those due to intrachain dipolar interactions.

The second, and more important, factor in the angular dependence of the line width in [Cu(dien)OAc](ClO_4), is that the angle between $\overline{AB}$, the nearest-neighbor vector in the chain, and the b axis is 16.4°. This means that the angular dependence of the line width depends greatly on θ', the angle between $\overline{AB}$ and the magnetic field direction ($\theta \neq \theta'$). The difference between the line width at $H \| a^\dagger$ and that at $H \| c$ can be explained by this fact as can the shift in the minima from the expected value of $\theta = 54.7°$ to $\theta \sim 60°$.

The single-crystal EPR spectra of [Cu(dien)OAc](ClO_4) give interesting results. There is sufficient interchain diffusion to give a Lorentzian line shape for all crystal orientations. This indicates a large amount of interchain-exchange coupling, which is confirmed, at least in the temperature range 5.0–60 K, by the large antiferromagnetic value of zJ'. The analysis of the angular dependence of the line width, however, showed that interchain dipolar coupling effects only small deviations from the expected one-dimensional behavior.

Intrachain next-nearest-neighbor antiferromagnetic exchange coupling could be an important contribution to zJ'. The dipolar contribution to the second moment from next-nearest neighbors in the chain results in a $\Delta H_{pp}(\theta)$ dependence that is predicted by eq 7, which is true for a "good" one-dimensional complex. This is because the angle between $\mathbf{r}_{ij}$ and the chain axis b is zero when i and j are next-nearest neighbors. Therefore, if next-nearest-neighbor intrachain-exchange coupling makes an important contribution to zJ', the angular dependence of the line width may be explained nicely. However, the Lorentzian line shape of the

(25) Weil, J. A.; Buch, T.; Clapp, J. E. *Adv. Magn. Res.* **1973**, *6*, 183.
(26) Waller, W. G.; Rogers, M. T. *J. Magn. Reson.* **1975**, *18*, 39.
(27) Hoffmann, S. K.; Corvan, P. J.; Singh, P.; Sethulekshmi, C. N.; Metzger, R. M.; Hatfield, W. E. *J. Am. Chem. Soc.* **1983**, *105*, 46808.
(28) Drumheller, J. E. *Magn. Reson. Rev.* **1982**, *7*, 123 and references therein.
(29) Dietz, R. E.; Merritt, F. R.; Dingle, R.; Hone, D.; Silbernagel, B. G.; Richards, P. M. *Phys. Rev. Lett.* **1971**, *26*, 1186.
(30) Richards, P. M. In *Low-Dimensional Cooperative Phenomena*; Keller, H. J., Ed.; Plenum: New York, 1974; p 147.
(31) Hennessy, M. J.; McElwee, C. D.; Richards, P. M. *Phys. Rev. B: Condens. Matter* **1973**, *7*, 930.
(32) Richards, P. M. In *Local Properties at Phase Transitions*; Mueller, K. A., Rigamonti, A., Eds.; Elsevier: Bologna, Italy 1975; p 539.

EPR spectra in all crystal orientations shows that there is a significant amount of interchain spin diffusion. This suggests that next-nearest-neighbor intrachain-exchange coupling is not the only contribution to zJ'.

The single-crystal EPR spectra and the crystal structure were obtained at room temperature, and the magnetic results were determined from data in the temperature region 5.0–60 K. Temperature-dependent interchain-exchange-coupling constants and crystal structure parameters have been observed,[5,24] and such phenomena could possibly be present in [Cu(dien)OAc](ClO$_4$). If this is true, contributions to the unusual behavior of the EPR spectra could arise from these effects. Low-temperature (<40K) single-crystal EPR spectra would be especially valuable for this complex. These measurements will be undertaken when the necessary equipment becomes available to us.

Acknowledgment. This work was supported in part by the National Science Foundation through Grant CHE 860 1438.

Registry No. [Cu(dien)OAc](ClO$_4$), 21279-30-1.

Supplementary Material Available: Listings of hydrogen atom positional parameters, anisotropic thermal parameters, and bond distances and bond angles in the diethylenetriamine ligand, the acetate ligand, and the perchlorate anion (4 pages); a listing of observed and calculated structure factors (8 pages). Ordering information is given on any current masthead page.

Contribution from the Laboratoire de Spectrochimie des Elêments de Transition, UA No. 420, Universitê de Paris-Sud, 91405 Orsay, France

Irregular Spin State Structure in Trinuclear Species: Magnetic and EPR Properties of $Mn^{II}Cu^{II}Mn^{II}$ and $Ni^{II}Cu^{II}Ni^{II}$ Compounds

Yu Pei, Yves Journaux, and Olivier Kahn*

Received July 16, 1987

In a dinuclear system AB where A and B are magnetic ions with local spins S_A and S_B, the spin multiplicity of the low-lying states monotonically varies versus the energy. The spin state structure is said to be regular. The $\chi_M T$ versus T plot (χ_M = molar magnetic susceptibility; T = temperature) continuously decreases or increases upon cooling down according to whether the interaction is antiferro- or ferromagnetic. In a linear trinuclear system ABA, the spin state structure is regular if $2S_A \leq S_B$ but otherwise becomes irregular. The spin multiplicity does not vary monotonically versus the energy anymore. When the A–B interaction is antiferromagnetic [$H = -J(S_{A1} \cdot S_B + S_{A2} \cdot S_B)$; $J < 0$], the ground state does not have the lowest spin if $2S_A > S_B + {}^1/_2$. This may lead to characteristic magnetic behavior with a minimum in the $\chi_M T$ versus T plot. Below the temperature of the minimum, the compound exhibits a ferromagnetic-like behavior. This behavior has been observed in two compounds, namely {Mn(Me$_6$-[14]-ane-N$_4$)]$_2$Cu(pba)}(CF$_3$SO$_3$)$_2$·2H$_2$O (**1**) and {[Ni(Me$_6$-[14]ane-N$_4$)]$_2$Cu(pba)}(ClO$_4$)$_2$ (**2**) with Me$_6$-[14]ane-N$_4$ = (±)-5,7,7,12,14,14-hexamethyl-1,4,8,11-tetraazacyclotetradecane and pba = propane-1,3-diylbis(oxamato). The magnetic properties of **1** and **2** have been quantitatively interpreted. **1**: $S = {}^9/_2$ ground state; $J = -36.6$ cm^{-1}. **2**: $S = {}^3/_2$ ground state with a zero-field splitting characterized by an axial parameter $|D| = 2.4$ cm^{-1}; $J = -124.5$ cm^{-1}. The X-band powder EPR spectrum of **1** shows the $\Delta M_S = \pm 1$ allowed transitions and the $\Delta M_S = \pm 2$ (and maybe also ± 3, ± 4) forbidden transitions within the $S = {}^9/_2$ state. The EPR spectrum of **2** at 5.8 K shows the transitions within the $\pm {}^1/_2$ Kramers doublet arising from the $S = {}^3/_2$ ground state. When the sample is warmed, a transition associated with the first excited doublet state appears.

Introduction

The field of molecular magnetism has known a rapid development in the last few years. It is perhaps not exaggerated to speak of a Renaissance of the field. It has already been emphasized that, among other reasons, this situation is due to the fact that this field lies at the meeting point of two apparently widely separated disciplines, namely molecular materials and bioinorganic chemistry.[1,2] As far as the field of molecular materials is concerned, one of the main challenges is the design of molecular ferromagnets. So far, several approaches have been proposed along this line,[3-5] and very recently the first genuine molecular systems ordering ferromagnetically have been reported.[6,7] One of the approaches consists first of synthesizing molecular entities with a large spin in the ground state and then of assembling them within the crystal lattice in a ferromagnetic fashion.[8-11] Recently, Iwamura et al. described polycarbene type molecules with a nonet ground state[8-10] and stressed that any other molecular system with such a high-spin multiplicity in the ground state did not exist so far. This result arises from the fact that eight electrons occupy eight quasi-degenerate molecular orbitals. Other strategies have been proposed to favor ferromagnetic interactions within a molecular entity, one of them being the orthogonality of the magnetic orbitals.[12] All require symmetry conditions that are often difficult to achieve. This is why we have decided to explore an alternative strategy allowing us to "throw off the yoke" of the symmetry requirements as much as possible, nevertheless leading to new molecular systems with a large spin in the ground state. This strategy is based on the concept of irregular spin state structure.

In the next section, we introduce the idea of spin state structure and the relation between the spin state structure and the magnetic behavior in the simple case of a dinuclear system; then we approach the case of a symmetrical trinuclear species, and we show that the spin state structure may be regular or irregular. In this latter

(1) See: *Magneto-structural Correlations in Exchange Coupled Systems*; Willett, R. D., Gatteschi, D., Kahn, O., Eds.; Nato ASI Series; Reidel: Dordrecht, The Netherlands, 1985; Series C, Vol. 140.
(2) Morgenstern-Badarau, I.; Cocco, D.; Desideri, A.; Rotilio, G.; Jordanov, J.; Duprê, N. *J. Am. Chem. Soc.* **1986**, *108*, 300.
(3) Kahn, O. *Angew. Chem., Int. Ed. Engl.* **1985**, *24*, 834 and references therein.
(4) Cairns, C. J.; Busch, D. H. *Coord. Chem. Rev.* **1986**, *69*, 1 and references therein.
(5) Breslow, R. *Pure Appl. Chem.* **1982**, *54*, 927.
(6) Pei, Y.; Verdaguer, M.; Kahn, O.; Sletten, J.; Renard, J. P. *J. Am. Chem. Soc.* **1986**, *108*, 7428.
(7) Miller, J.; Calabrese, J. C.; Epstein, A. J.; Bigelow, R. W.; Zhang, J. H. *J. Chem. Soc., Chem. Commun.* **1986**, 1026.
(8) Iwamura, H.; Sugawara, T.; Itoh, K.; Takui, T. *Mol. Cryst. Liq. Cryst.* **1985**, *125*, 251.
(9) Sagawura, T.; Bandow, S.; Kimura, K.; Iwamura, H.; Itoh, K. *J. Am. Chem. Soc.* **1986**, *108*, 368.
(10) Teki, Y.; Takui, T.; Itoh, K.; Iwamura, H.; Kobayashi, K. *J. Am. Chem. Soc.* **1986**, *108*, 2147.
(11) Pei, Y.; Kahn, O.; Sletten, J. *J. Am. Chem. Soc.* **1986**, *108*, 3143.
(12) Kahn, O.; Galy, J.; Journaux, Y.; Jaud, J.; Morgenstern-Badarau, I. *J. Am. Chem. Soc.* **1982**, *104*, 2165.

0020-1669/88/1327-0399$01.50/0